Tensor polarization in pion-deuteron elastic scattering

E. Ungricht,* W. S. Freeman,† D. F. Geesaman, R. J. Holt, J. R. Specht, and B. Zeidman
Argonne National Laboratory, Argonne, Illinois 60439

E. J. Stephenson
Indiana University Cyclotron Facility, Bloomington, Indiana 47405

J. D. Moses
Los Alamos National Laboratory, Los Alamos, New Mexico 87545

M. Farkhondeh, S. Gilad, and R. P. Redwine
Massachusetts Institute of Technology, Cambridge, Massachusetts 02139
(Received 1 November 1984)

Angular distributions of the deuteron tensor polarization, t_{20}, in π-d elastic scattering have been measured at pion energies of 180, 220, and 256 MeV. The experiment and analysis are described in detail. Theoretical calculations in which the effects of pion absorption on the elastic channel are small seem to reproduce the data. An excitation function was measured in order to search for a rapid energy dependence of t_{20}. No rapid angular or energy dependence was found near a pion energy of 134 MeV, where other experiments have suggested the existence of dibaryon resonances.

I. INTRODUCTION

During the past few years, interest in the pion-deuteron system has been spurred by questions regarding the existence of dibaryon resonances, true pion absorption in nuclei, and the quadrupole form factor of the deuteron. Early calculations indicated that a measurement of tensor polarization t_{20} in π-d scattering should give an accurate determination of the quadrupole form factor and therefore the D-state probability of the deuteron.[1] Subsequent calculations showed that the effects of pion absorption were not completely understood[2–6] and that absorption had a profound influence on the tensor polarization. Presently, the theoretical calculations of the π-d system have achieved a high level of sophistication. The three-body calculations are relativistic and include pion absorption. There is an urgent need for precise data to check the theoretical predictions. While extensive measurements of cross sections[7–9] and vector polarizations[10,11] are published, this is the first extensive measurement of tensor polarizations over a broad range of energies at and above the Δ-resonance region. The present data show that the effects of pion absorption on the elastic observables may be smaller than expected.

Recent measurements[12] of t_{20} from SIN show a rapid angular and energy dependence, which is interpreted as evidence for dibaryon resonances. Their results disagree with previous measurements[13] from our collaboration, but they are so striking and unexpected that they should be reexamined. Our new data contradict the SIN measurements and confirm the trends of our previous measurements, thus showing no evidence for resonancelike structures. Since this disagreement with the SIN measurements persists, we discuss the present experiment in detail in Sec. II; the data are presented in Sec. III.

II. EXPERIMENTAL METHOD

The π-d scattering experiment was performed[14] at the P^3 channel of the Clinton P. Anderson Meson Physics Facility with the setup shown schematically in Fig. 1. After the π^+ beam interacted with a liquid deuterium target, the elastically scattered pions and the recoiling deuterons were detected in coincidence. The deuterons were focused by a quadrupole doublet and momentum analyzed in a dipole magnet before entering the polarimeter; the pions were identified in a telescope consisting of three plastic scintillators.

The properties of the pion beam, the deuterium target, and the magnetic spectrometer are discussed in the following subsection. To a large extent, these properties are determined by the polarimeter design which is presented in the second subsection.

A. Pion beam, deuterium target, and magnetic spectrometers

Since the deuteron tensor polarimeter was calibrated in a separate experiment at the Berkeley 88-inch cyclotron, it was necessary to ensure that the deuterons from the present π-d scattering experiment fell in the same spatial and energy range as those in the calibration. Thus, special care was taken in order to tailor the incident pion beam quality, deuterium target thickness, spectrometer tune, and deuteron beam degraders so that the deuterons incident on the polarimeter at Los Alamos Meson Physics Facility (LAMPF) were consistent in energy and trajectory with those in the calibration. The two X-Y wire chambers and the Si(Li) detectors located in front of the polarimeter (see Fig. 1) were used to verify the trajectories and energy distribution of the incident deuteron beam before each data point was recorded.

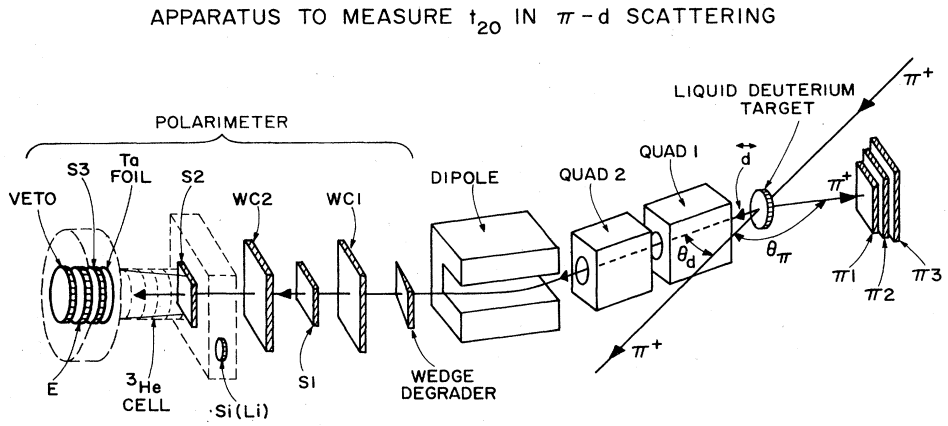

FIG. 1. Schematic diagram of the experimental setup to measure t_{20} in π-d scattering.

The energy and position distributions of the deuterons entering the polarimeter were strongly affected by the target thickness, the size of the energy degrader needed to match the deuteron energy to the polarimeter acceptance, the momentum resolution of the pion beam, and the pion beam spot size. These were optimized for each pion energy and scattering angle with the help of a computer program that took into account beam optics up to second order for the deuteron arm and energy loss and multiple-scattering effects in the target, the vacuum windows, and the degrader. A 4% total momentum was used for the pion channel whenever possible in order to maintain a high event rate. However, near 140 MeV, this momentum spread was reduced to 2% so that there would be sufficient resolution to observe a rapid energy dependence in t_{20}. The pion beam energies were taken from the channel optics and are believed[15] to be reliable to 1 MeV. The pion beam spot size was 20 mm (FWHM), and was continuously monitored with a wire chamber profile monitor mounted in place of the target for tune up, and just in front of the target during runs. The pion beam intensity was verified by $^{12}C(\pi,\pi'N)^{11}C$ activation measurements.[16]

The liquid deuterium target was chosen to be 5-mm thick. Together with the selected pion momentum width, this resulted in a deuteron energy distribution 2.5 to 3 MeV wide just after the target. The target was mounted in a vacuum can and rotated to the position for optimum deuteron energy resolution at each scattering angle. The target frame was much larger than the beamspot (80 vs 20 mm diameter) so that scattering from the frame was negligible. A uniform target thickness was maintained by using very thin double foils (0.13+0.05 mm Mylar) to contain the deuterium; the space between the inner and outer foil was filled with gaseous deuterium at the same pressure as the liquid deuterium to prevent the windows of the liquid target from bulging outward. An empty target cell identical to the full cells was used to check the background at several angles and energies. The background was always found to be negligible. The measurement at a pion energy of 180 MeV and a deuteron scattering angle of 30° was performed with a solid CD_2 target because of a failure in the liquid deuterium target. The parameters for the experimental configurations are given in Table I.

Care was taken to minimize the number of deuterons or protons from sources other than the target. Protons in the pion beam were eliminated with a CH_2 and Be degrader located between two of the bending magnets in the P^3 channel. The proton contamination of the pion beam was then negligible.[15] The pion beam passed through thin windows only, making the total mass in the pion path before or near the target comparable to the target mass. After the target, the pion beam passed through a Kapton window into air and was stopped in Pb located 8 m behind the target. The scattered pions left the target can through the 3-mm aluminum wall and were detected in a telescope of three scintillators, each 3 mm thick ($\pi 1$-$\pi 3$ in Fig. 1). Protons were eliminated by the target can and by a 13-mm aluminum plate between the first and second scintillator. The solid angle of the pion telescope was sufficiently large (30 msr) so that the overall solid angle was defined by the recoil deuteron channel.

The recoiling deuterons left the target can through a 0.08-mm Kapton window, passed through a 40-mm air gap, and entered the magnet vacuum channel through another 0.08-mm Kapton window. The deuterons were focused by a quadrupole doublet and momentum analyzed by a dipole magnet with a 35° bend angle before they entered the front end of the polarimeter through a 90-mm air gap. Energy degraders were inserted into the two air gaps before and after the magnets so that the deuteron energy distribution matched the polarimeter acceptance. The solid angle of the deuteron channel was defined by a pair of vertical and horizontal slits (25-mm thick steel) before the first quadrupole magnet, and was set to 8.5 msr with a horizontal and vertical acceptance of $\pm 1.5°$ and $\pm 4.5°$, respectively. A second pair of slits after the dipole magnet reduced and background from particles scattered by the vacuum chamber walls.

B. Polarimeter

The key feature for performing measurements of t_{20} in π-d scattering is the development of a high-quality deute-

TABLE I. Experimental parameters for π-d scattering (present experiment).

Pion energy (MeV)	Momentum bite (%)	Pion flux (s^{-1})	Target thickness (mg/cm^2)[a]	Deuteron angle (deg)	Recoil energy (MeV)	Deuteron at polarimeter energy (MeV)	Deuteron at polarimeter width (FWHM) (MeV)
142 (π^-)	4		82	0	48.8	23.1	3.2
134	2	0.7×10^8	95	18	41.1	24.0	2.1
142	2		86	18	44.1	23.4	2.5
151	2		88	18	47.5	23.9	2.7
180	2	2×10^8	86	18	59.1	23.5	3.1
180	4		196[b]	30	48.9	23.7	3.5
180	4		57	44	33.6	23.7	2.8
220	4		86	18	76.1	22.8	4.0
220	4		114	44	43.2	22.9	3.2
256	4	8×10^8	86	18	92.3	21.9	5.5
256	4		95	30	76.2	22.0	5.0
256	4		114	44	52.3	23.1	4.0

[a]Liquid D_2 target with density 0.163 g/cm^3.
[b]Solid CD_2 target.

ron tensor polarimeter. The polarimeter must have not only a high efficiency and analyzing power, but also a large radial, angular, and energy acceptance for the deuterons and good background suppression. Since the recoiling deuteron beam energy changes drastically for different pion energies and π-d scattering angles, it is necessary to measure the energy and spatial parameters of the deuteron beam and to calibrate the polarimeter as a function of these parameters.

The ^{3}He(**d**,p)^{4}He reaction was chosen as the analyzing reaction for the deuteron tensor polarization t_{20} because of its large cross section and tensor analyzing power in the forward direction and because of the large positive Q value, 18.4 MeV. The cross section for this reaction can generally be written as

$$\frac{d\sigma}{d\Omega}=\frac{d\sigma_0}{d\Omega}[\,1+2iT_{11}\mathrm{Re}(it_{11})+T_{20}t_{20}+2T_{21}\mathrm{Re}(t_{21})+2T_{22}\mathrm{Re}(t_{22})]\,,$$

where $d\sigma_0/d\Omega$ is the cross section for unpolarized deuterons. If the polarimeter and the deuteron beam are rotationally symmetric about the beam axis, all polarization effects other than those due to t_{20} cancel with integration over the proton solid angle. The deuteron polarization t_{20} and the polarimeter analyzing power T_{20} are the related by

$$\epsilon=\epsilon_0(1+t_{20}T_{20})\,,$$

where the efficiency ϵ is defined as the ratio of outgoing protons to incoming deuterons, and ϵ_0 is the efficiency of the polarimeter for unpolarized deuterons. The efficiencies and the analyzing power are in principle complicated functions of the energies and trajectories of the incoming deuterons. Consequently, we took care to measure the trajectories and energy spectra of the deuterons during the calibration procedure.

The basic features of the new polarimeter were very similar to those of the prototype[17] used to measure t_{20} at $\theta_d=0°$. Time-of-flight measurements over a 3.7-m path and energy-loss signals from a high-quality scintillation system allowed a good separation of deuterons and protons from background. A large ^{3}He gas region gave a good spatial and angular acceptance while essentially complete transmission of the deuterons through the active volume was ensured. Accurate measurements of energies and trajectories of the deuterons were used for comparison with calibration data. The effective efficiency and analyzing power of the polarimeter were $\epsilon_0\approx1\times10^{-4}$ and $T_{20}\approx-0.6$, respectively. Prior to the present experiment, the same polarimeter was used in measurements of the tensor polarization in π-d scattering[13] at 142 MeV and in e-d elastic scattering.[18]

A cross-section view of the polarimeter along the beam axis is shown in Fig. 2. A 0.25-mm titanium foil with 89 mm diameter served as entrance window into the 12° conical ^{3}He cell. The active volume was 35-cm long, corresponding to a ^{3}He areal density of 96 mg/cm^2 at the operating pressure of 22 bar.

A deuteron was identified by requiring correct energy-loss signals in the 0.8-mm thick transmissions scintillators $S1$ and $S2$, and by the time difference between the pion signals in $\pi1\cdot\pi2\cdot\pi3$ and the deuteron signal in $S2$. The entrance window defined the active diameter, and the position of $S2$ mounted behind the window defined the beginning of the active ^{3}He region. Two wire chambers WC1 and WC2 were used to measure the trajectory of each deuteron. Before and after each polarization mea-

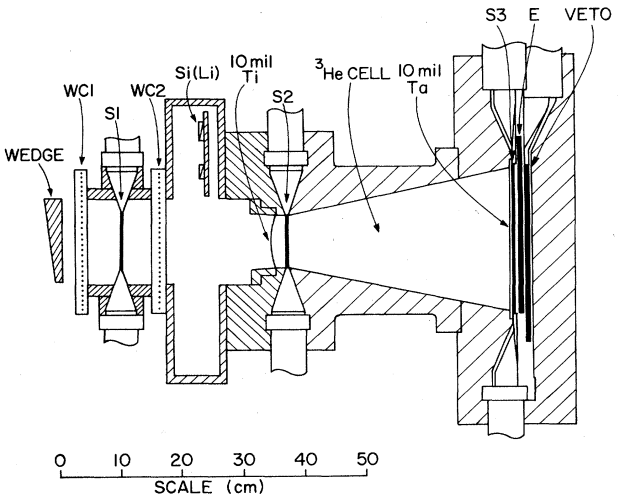

FIG. 2. Cross section of polarimeter along deuteron path.

surement two 5-mm thick Si(Li) semiconductor detectors were moved into the deuteron beam to map its position-dependent energy distribution with an intrinsic resolution of ± 70 keV (FWHM). ^{241}Am was deposited on the surface of the detectors in order to give an absolute energy calibration reproducible to $\pm 1\%$. The entire front end of the polarimeter from WC1 to the titanium entrance window was filled with ^{4}He at atmospheric pressure to minimize the energy loss.

A proton from the ^{3}He(**d**,p)^{4}He reaction was identified by correct energy loss and energy signals in the scintillators $S3$ and E (2.4 and 9.5 mm thick), and by correct time of flight through the polarimeter between $S2$ and $S3$. A 6.4-mm thick veto scintillator eliminated protons with too much energy. The E detector was split into four segments in order to give left-right and up-down information and was used to check for systematic errors. Each of the thin scintillators ($S1$,$S2$,$S3$) was coupled to two phototubes to improve the uniformity of the light collection and consequently the energy resolution. For ^{3}He(d,p)^{4}He reactions taking place near the front of the active ^{3}He volume, the solid angle for protons was determined by the rear opening in the conical gas cell. Reactions taking place at lower energy near the rear of the gas cell were not limited by this cone, but by the increasing energy loss in the $S3$ counter as the scattering angle increased. Thus, protons from the ^{3}He(d,p)^{4}He reaction are present down to zero pulse height in the E-counter spectrum. The solid angle depends in part on the E-counter threshold, which was kept at a fixed fraction of the ^{241}Am source line in both the Berkeley calibration and data acquisition at LAMPF. In addition, the $S3$ and E counters were left in place between the calibration and all experiments to maintain a constant geometry.

Energy thresholds and gains were determined with $\sim 5\%$ precision from the data by examining the spectra for fast protons produced in the target and stopped in the E detector. The spectra showed a sharp upper edge, corresponding to the energy where the range exceeded the thickness of the E detector and a veto signal was produced. This energy was easily calculated independent of all other experimental conditions.

Unfortunately, a small amount of helium gas diffused through the lucite windows and the glass walls into the photomultipliers. The photomultiplier tubes were protected by blowing air over the sides, but even then the amplification gradually changed and had to be readjusted daily. After a few weeks of operation, some of the tubes finally failed due to helium damage and had to be replaced. An accurate energy calibration was obtained from weak alpha sources (^{244}Cm) painted onto the scintillators, and from the energy-loss signals of fast protons passing through the thin detectors.

A 0.25-mm tantalum foil in front of $S3$ stopped all deuterons to reduce the count rate in $S3$. The thickness of the tantalum foil and the $S3$ detector was chosen such that no proton produced by a deuteron with energy below 3 MeV reached the E detectors. Therefore, the polarimeter was not sensitive to the 430 keV resonance in the ^{3}He(d,p)^{4}He reaction. Protons produced by deuterons with an energy above 29 MeV at the Si(Li) detectors did not stop in the E detectors and produced a veto signal. Thus, we chose 29 MeV to be an upper limit for the energy of deuterons incident at the location of the Si(Li) detectors.

The calibration parameters for the efficiency ϵ_0 and tensor analyzing power T_{20} were obtained by extensive measurements with a polarized deuterium beam from the Berkeley cyclotron. In two repeated measurements the beam energy was varied in 0.5 MeV steps for a centered beam (Fig. 3). The response for twelve different off-center beam positions was obtained at three energies, and the effects of tilting the polarimeter was measured at three energies and four positions for two angles each (Fig. 4). During these measurements the beam polarization was continuously monitored with a ^{4}He(**d**,d)^{4}He polarimeter[19] which was operated constantly at 35 MeV beam energy. Two years later and just preceding the present work, the most crucial calibration, the dependence of the efficiency on the deuteron energy, was repeated at the Los Alamos three-stage tandem accelerator. At that time a better energy calibration procedure was found and it was subsequently applied as a correction to the Berkeley data. A second correction came from a small ^{3}He pressure difference between the two experiments and was obtained from pressure measurements and a model calculation of the polarimeter. The two calibrations agreed within $\sim 2\%$ (Fig. 3). The calibration data for ϵ_0 (E,**x**) and T_{20} (E,**x**) were described by a function of four spatial coordinates and the energy of the deuteron as

$$f(E,\mathbf{x}) = f_E(E) + f_x(x,\theta,E) + f_y(y,\theta,E) + f_{xy}(x,\theta,y,\phi,E) .$$

The first term carries the energy dependence as a piecewise-continuous cubic polynomial. Off the central axis, f_x and f_y include quadratic variations in **x** and f_{xy} includes linear correlations.

Even with such a highly efficient polarimeter, the pro-

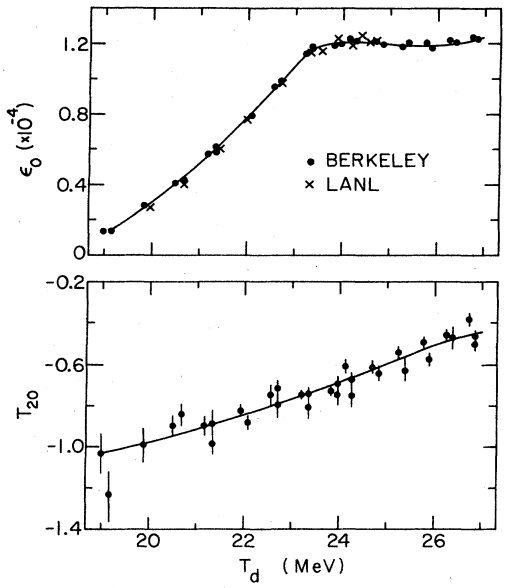

FIG. 3. Energy dependence of the polarimeter calibrations ϵ_0 and T_{20}. Solid points are Berkeley data (1980), crosses are Los Alamos data (1982).

ton count rates from ^{3}He(d,p)^{4}He were still very low and allowed only a measurement of the averaged polarized efficiency

$$\langle \epsilon \rangle = \langle \epsilon_0 \rangle \left[1 + t_{20} \frac{\langle \epsilon_0 T_{20} \rangle}{\langle \epsilon_0 \rangle} \right].$$

Here, the quantities in parentheses are averaged over the position and energy distribution of the incident deuteron beam. The deuteron flux, however, was measured as a function of five parameters describing the energy and trajectory. This flux measurement for each run was used as a weighting function in producing the average values $\langle \epsilon_0 \rangle$ and $\langle \epsilon_0 T_{20} \rangle$ from the Berkeley calibration data for ϵ_0 and T_{20}. A π-d scattering measurement consisted of a deuteron-beam optimization, a deuteron-beam scan to obtain the weights for $\langle \epsilon_0 \rangle$ and $\langle \epsilon_0 \cdot T_{20} \rangle$, a polarization run to obtain $\langle \epsilon \rangle$, and finally another deuteron-beam scan to check the first one.

The magnetic spectrometer combined with carefully adjusted wedge-shaped absorbers produced a deuteron-beam distribution (see Fig. 5) with very small correlation between energy and trajectory at the polarimeter entrance. The size and angular spread (Fig. 6) of the deuteron beam was monitored continuously. The energy spread was minimized for each measurement, but a broader deuteron spectrum was inevitable at higher pion energies. The absorbers were always chosen such that there were no deuterons above 29 MeV at the Si(Li) detectors (Fig. 7 and Table I).

As mentioned earlier, the same polarimeter was used in an e-d scattering experiment[18] where the background problems were much more severe. The results of that experiment agreed with reliable theoretical calculations, thereby providing additional confidence in the calibration and operation of the polarimeter.

C. Data acquisition and reduction

Since the pion beam produced more background protons than elastically scattered deuterons and the ^{3}He(**d**,p)^{4}He polarimeter had an efficiency of about 1×10^{-4}, a background suppression of 10^{-6} was needed. This was possible with the setup and the polarimeter described here.

Events were defined electronically by first establishing a "pion" as a coincidence $\pi1\cdot\pi2\cdot\pi3$, a "deuteron" as a coin-

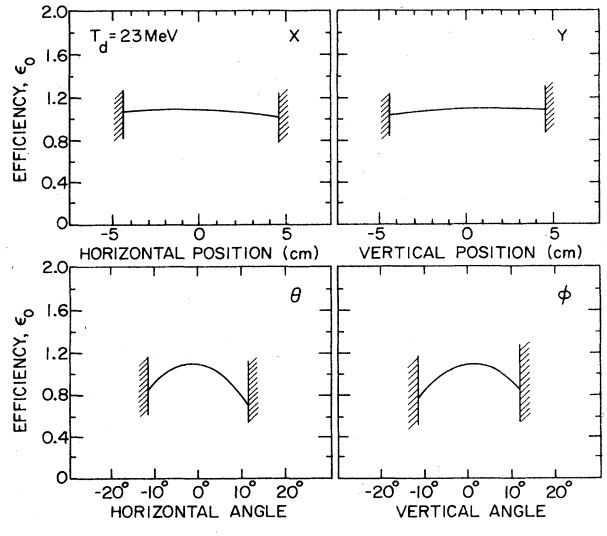

FIG. 4. Position and angle dependence of the polarimeter efficiency ϵ_0 derived from the Berkeley calibration at 23 MeV deuteron energy.

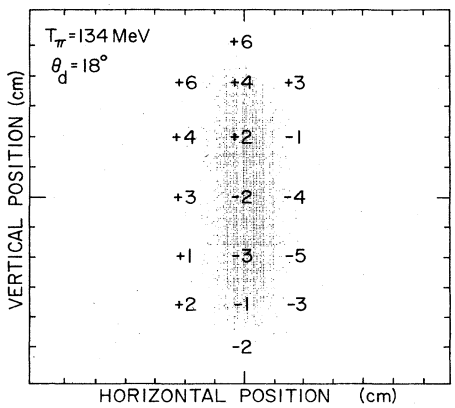

FIG. 5. Typical energy variation across the deuteron beam (in 100 keV units), as measured with the Si(Li) detectors. The dots show the intensity distribution of the beam.

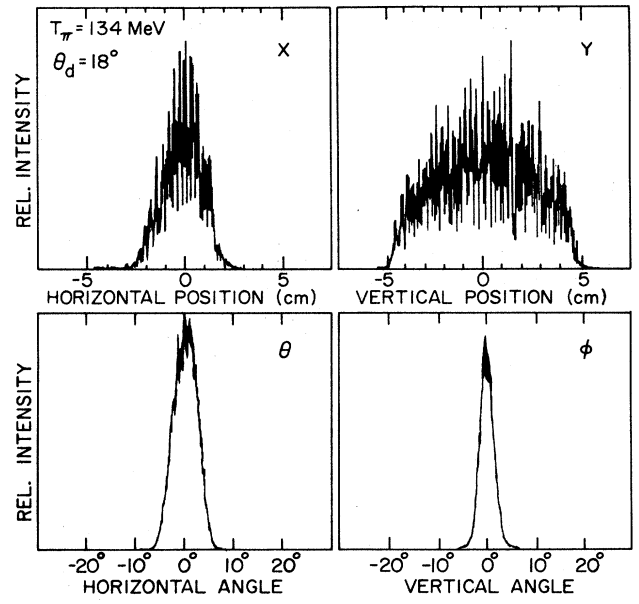

FIG. 6. Typical horizontal and vertical deuteron beam profile (top: position; bottom: angle), as measured with the wire chambers.

cidence $S1 \cdot S2$, and a "proton" as a coincidence $S3 \cdot E$. Either "pion-deuteron" or "pion-deuteron-proton" coincidence generated an event-trigger for the computer. There were, of course, many deuterons which produced no proton in the polarimeter so that $S3$ and E registered no particle. Such events were prescaled by a factor of 100 to keep the computer dead time low. Events were accepted only during a beam spill and if the veto detector had no signal. The electronic coincidence widths were wide (20—60 ns) and the discriminator thresholds were much lower than the signals, so that software windows could be used later. The final selection was done with digitized pulse height and timing signals as described in the following. For each event, 25 parameters were recorded. The most important were three energy losses from the pion telescope; two energy losses from the deuteron; energy loss and energy from the proton; three time differences $S1$-$S2$, $S2$-$S3$, and π-$S2$; and eight time signals from the delay-line wire chambers.

The events were then analyzed by a series of one- and two-dimensional filters. A background correction (less than 2%) was applied to all filters containing timing information; rates were sufficiently low that no correction was necessary for the dead time of the time-to-digital converters. A deuteron from π-d scattering was identified by the energy loss in $S1$ and $S2$ (Fig. 8) and the time difference π-$S2$ corresponding to the 3.7-m flight path of the deuteron from the target to the polarimeter. A proton produced in the polarimeter by such a deuteron was subsequently identified by the time of flight through the polarimeter, $S2$ to $S3$, vs the proton energy E (Fig. 9) and the energy loss $S3$ vs energy E. Then the final threshold was applied to the energy spectrum. At lower pion energies, the last software cuts on $S3$ and E were found to be redundant; at very high energy (256 MeV) and forward angles (18°), however, they were needed.

As mentioned earlier, the deuteron beam was scanned with Si(Li) detectors to get a high-resolution energy spectrum. The scans were normalized to the primary beam intensity on the pion production target. The measurements were analyzed with a filter on the energy loss in $S1$, the energy in the Si(Li), and the time difference π-$S1$. The five parameters describing energy and trajectory of each deuteron were then used to obtain the average efficiency $\langle \epsilon_0 \rangle$ and analyzing power $\langle \epsilon_0 \cdot T_{20} \rangle$.

Before each analysis the raw spectra were inspected and it was verified that all discriminator thresholds were suffi-

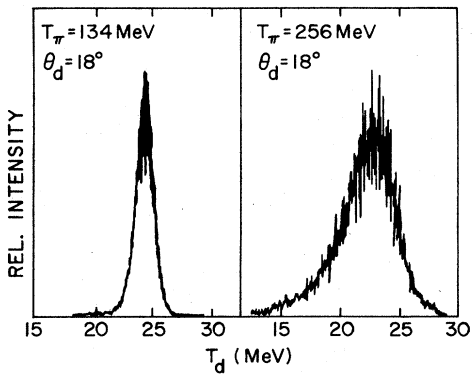

FIG. 7. Deuteron beam spectra after wedge degraders for low and high pion energies. The deuteron energy is measured with the Si(Li) detectors.

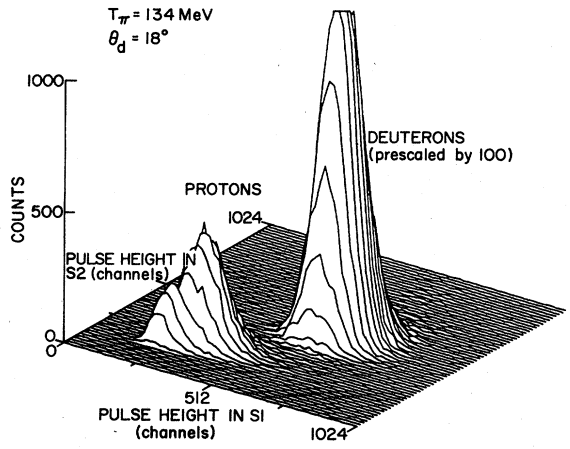

FIG. 8. Typical deuteron energy loss spectrum $S1 \times S2$ (raw data). All of the protons have generated a "πdp" signal and are therefore not prescaled, while the deuterons are prescaled by 100.

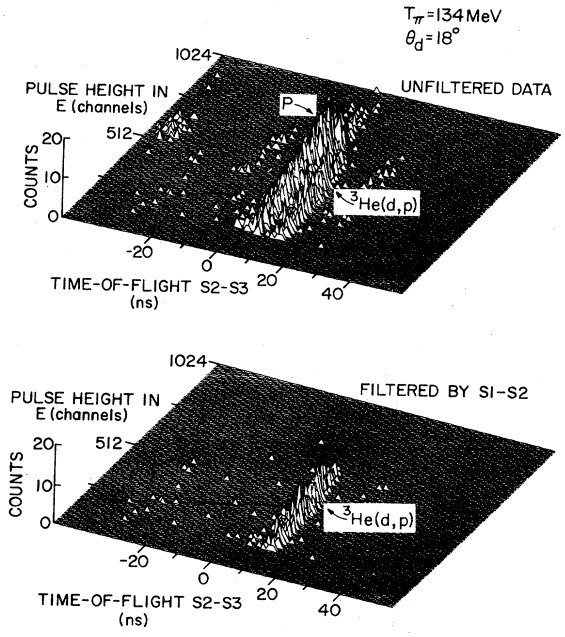

FIG. 9. Typical spectrum for time of flight through the polarimeter $S2$-$S3$ vs proton energy E. The effect of the $S1 \cdot S2$ filter is demonstrated by the difference between the unfiltered (top) and filtered data (bottom). Both spectra have a 15 ns window on the deuteron time-of-flight π-$S2$.

ciently low. The deuteron beam profiles from the two wire chambers were checked for unfiltered and filtered events. These checks showed some beam position fluctuations of approximately a millimeter for the early data. This small movement of the deuteron beam was attributed to a poor stabilization of the dipole magnet power supply. After the power supply was repaired, a repetition of the affected measurements confirmed the earlier measurements of t_{20}. Since the experiment was split into two parts, the reproducibility could be checked over a two-month period. All repeated data points agreed well within the statistical errors.

For each measurement, the symmetry of the deuteron beam was checked with the wire chambers. As shown in Fig. 6, the intensity distribution is not rotationally symmetric about the polarimeter axis; its elliptical shape suggests sensitivity to a t_{22} moment in the deuteron beam. The simple formula for efficiency, $\epsilon = \epsilon_0(1 + t_{20}T_{20})$, will not be accurate if the t_{22} beam moment is large and the elliptical spot distribution introduces a significant T_{22} analyzing power for the polarimeter. This problem should, however, reveal itself first in a difference between the sum of up and down compared with the sum of left and right segments of the E counter. To within statistics, no such difference was observed. Moreover, the T_{22} analyzing power of the polarimeter was determined to be <0.05 during the calibration procedure. Finally, the effects of other filters or different filter sequences on the data was also checked. All data were analyzed with three different filters called wide, optimal, and narrow. The results from the wide and optimal filters agreed after background subtraction, while the narrow filters sometimes eliminated good events.

D. Error analysis

For the error analysis, the errors were separated into two groups: relative errors that changed for each data point and systematic errors that changed from experiment to experiment only (e.g., between the calibration at Berkeley, the calibration at the Los Alamos tandem, and the π-d experiment at LAMPF). Contributions to the relative errors came from deuteron and proton counting statistics, uncertainties in deuteron energies due to fluctuations in beam and Si(Li)-energy calibration, fluctuations in the gain and threshold calibration of the E scintillators, and uncertainties in the ^{3}He pressure; the two biggest contributions came from the proton counting statistics and deuteron energy fluctuations. All relative errors were added quadratically to give

$$(\Delta t_{20})^2_{\text{rel}} = t_{20}^2 \sum \left[\frac{\Delta T_{20}}{T_{20}}\right]^2 + \left[t_{20} + \frac{1}{T_{20}}\right]^2 \times \sum \left[\left[\frac{\Delta\epsilon}{\epsilon}\right]^2 + \left[\frac{\Delta\epsilon_0}{\epsilon_0}\right]^2\right],$$

where the sums cover all contributions to the error. The systematic errors were dominated by the absolute Si(Li)-energy calibration for the deuteron beam measurement which resulted in partially compensating errors in ϵ_0 and T_{20} and represented by $(\Delta t_{20})_{\text{correl}}$ in the following. Other error sources were the absolute pressure calibration, the scintillator gain matching between experiments, the uncertainty of the beam polarization in Berkeley, and the uncertainty of the parameters fitted to the Berkeley calibration. It was unlikely that all six sources of systematic errors would point in the same direction, so the errors were added quadratically, but in order to account for such a small sample, a tolerance factor f_{tol} of 1.5 was included to give a 70% probability that the calculated error was equal or bigger than one standard deviation:

$$(\Delta t_{20})_{\text{sys}} = f_{\text{tol}} \left[(\Delta t_{20})^2_{\text{correl}} + t_{20}^2 \sum \left[\frac{\Delta T_{20}}{T_{20}}\right]^2 + \left[t_{20} + \frac{1}{T_{20}}\right]^2 \sum \left[\frac{\Delta\epsilon_0}{\epsilon_0}\right]^2\right]^{1/2}.$$

E. Zero-degree measurement

As a feasibility test, a measurement at $\theta_d = 0°$ was attempted, even though the experimental setup was not designed originally for such an angle. The pions were scattered backwards into the incoming beam and could not be detected, thus reducing the available deuteron time-of-flight path drastically, since the 0.25 m between $S2$ and $S3$ had to be used in place of the 3.7 m between π and $S2$.

The pion beam was switched from π^+ to π^- so that the dipole magnet bent the negative pions through a 5-mil Kapton window into air, away from the polarimeter. In addition, it was expected that the quasielastic π-p scattering from the target should be approximately nine times smaller for π^- than for π^+. Nevertheless, a very high proton rate from the windows of the target and vacuum chamber made background elimination difficult. The data were analyzed with the same filters as the other measurements. These filters worked very well for a test measurement at 180-MeV pion energy and 18° deuteron angle with the π-d coincidence requirement removed from the electronics, thus indicating that the analysis was basically correct. However, the background, its uncertainty, and the effects of variations in the software window sizes were much bigger for the zero-degree measurement, resulting in a much larger error. The final result differs by slightly more than the error bar from an old data point[9] which was measured with a very different setup and the prototype of the present polarimeter.

TABLE II. Tensor polarization t_{20} in π-d scattering. In addition to the individual errors quoted for each data point (which include counting statistics and other fluctuating error sources) there is a systematic uncertainty of $\Delta t_{20} \approx \pm 0.1$ for each experiment.

Present experiment (1983)		
T_π^{lab} (MeV)	θ_d^{lab} (deg)	$t_{20}^{lab} \pm \Delta t_{20}$ (After 35° bend)
134	18	−0.62±0.10
142	0	−0.64±0.23
	18	−0.65±0.08
151	18	−0.64±0.10
180	18	−1.00±0.11
	18	−1.06±0.18
	30	−0.61±0.10
	44	−0.44±0.08
220	18	−1.28±0.15
	44	−0.34±0.08
256	18	−0.98±0.13
	30	−0.77±0.13
	44	−0.46±0.12
	44	−0.36±0.14

Earlier experiments (Refs. 9 and 13) (1978, 1980)		
T_π^{lab} (MeV)	θ_d^{lab} (deg)	$t_{20}^{lab} \pm \Delta t_{20}$ (Without bend)
142	0	−0.23±0.15
142	17.5	−0.40+0.10/−0.20
	28.9	−0.47+0.10/−0.16
	40.9	−0.44±0.11

III. RESULTS AND DISCUSSION

The results from the present work and from previous experiments by the same group[9,13] are summarized in Table II. Note that the quoted errors for each data point include counting statistics and other relative error sources as discussed earlier. In addition, there is a systematic uncertainty of $(\Delta t_{20})_{sys} \approx \pm 0.1$ for each of the three experiments. Any systematic correction within this range will be the same for all data points taken during one experiment. A check of our previous data[13] showed some problems caused by a high threshold in the $S3$ counter at $\theta_d = 17.5°$ and 28.9°. Therefore the error bars for these two points were changed to larger and asymmetric values.

The data from the present work give the tensor polarization in the laboratory system after a 35° bend in the dipole magnet; the old data do not have this rotation. In order to compare theoretical calculations with the experiment, calculated values of the tensor polarizations, $t_{20}^{c.m.}$, $t_{21}^{c.m.}$, and $t_{22}^{c.m.}$, have to be transformed from the center-of-mass system to the laboratory frame, including precession in the dipole magnet when necessary. When the coordinates are chosen according to the Madison convention[21] with the Z axis along the outgoing deuteron momentum, the transformations are

$$t_{20}^{lab} = \tfrac{1}{2} t_{20}^{c.m.} (3\cos^2\beta - 1) - 2\sqrt{(3/2)} t_{21}^{c.m.} \sin\beta\cos\beta + \sqrt{(3/2)} t_{22}^{c.m.} \sin^2\beta ,$$

$$\beta = \theta_{lab}^{d} - \theta_{c.m.}^{d} + \theta_{bend}^{d} \frac{E_d}{M_d} (1 - \mu_d) ,$$

$$\cos\theta_{lab}^{d} = \hat{k}_{in}^{\pi} \cdot \hat{k}_{out}^{d} .$$

The total energy, rest mass, and magnetic dipole moment of the deuteron are denoted by E_d, M_d, and μ_d. The kinetic energy of the deuterons in the bending magnet is about 40 MeV. Unfortunately, most calculations define the Z axis along the outgoing pion momentum, indicated by a positive $t_{21}^{c.m.}$ at small angles. This frame can be transformed to the Madison frame in the center of mass by

$$t_{kq}^{d} = (-1)^q t_{kq}^{\pi} .$$

A. Comparison with SIN data

A group at SIN (Ref. 12) measured the tensor polarization for pion-deuteron scattering in the region of 120—160 MeV pion energy. They found a resonancelike structure in the excitation function and strongly oscillating angular distributions at resonance energy. Some of their data are compared with the present results in Fig. 10. Because of placement of the pion telescope, the present setup did not allow measurements at $\theta_d = 15°$ where the SIN group found a pronounced peak, but with the angular distributions reported in that work, there should be some structure visible at $\theta_d = 18°$. Clearly, the present work shows no structure around 140-MeV pion energy and, in addition, gives much more negative values for the tensor polarization. Note that the discrepancy between the present work and that of Ref. 12 cannot be accounted for by the fact that the rotation angles β for the two experiments are different. The effect of the additional 35° bend of the deuteron beam in the present experiment is small. In fact, the additional precession angle introduced by the 35° bend is only 5°. The curves shown in the figure represent the theoretical calculations of Garcilazo[22] and Matsuyama and Lee.[23]

Although the exact cause of the discrepancy has not yet been determined, it is useful to compare the two experiments in more detail. The main differences reside in the polarimeter designs. First, the aperture of the SIN polarimeter (3.0 cm) is approximately three times smaller than that of our polarimeter (8.9 cm). Since the deuteron beam size at SIN is comparable with the polarimeter aperture, it is possible that particles identified as deuterons entering the polarimeter hit a wall and never entered the ^{3}He volume. This would have resulted in a low efficiency ϵ and a more positive t_{20}^{lab}. Since the deuteron trajectories were not measured in the SIN experiment, this effect might lead to the observed disagreement. This problem is avoided in our experiment in two ways: (i) the aperture of the polarimeter is approximately three times larger as mentioned, and (ii) two x-y wire chambers measure the trajectory of each deuteron entering the polarimeter. Also, the wire chambers are used at the beginning of each run in order to tune the quadrupole-quadrupole-dipole (QQD) system and to align the polarimeter with respect to the deuteron beam. Secondly, in the present experiment the energies of the deuteron incident on the polarimeter are measured by scanning the polarimeter aperture with Si(Li) detectors. The importance of measuring the deuteron energy accurately can be seen from the rapid energy dependence of ϵ_0 in Fig. 3. In the SIN experiment, the deuteron energies are determined by allowing the deuterons to range out in aluminum foils. Although this method is generally accepted for finding the centroid of the deuteron energy spectrum, it is difficult to determine the spectrum of deuteron energies. This is important since the width of the deuteron energy spectrum at $T_d = 20$ MeV is typically 6 MeV in the SIN experiment.

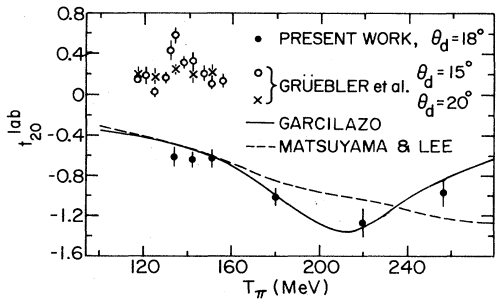

FIG. 10. Excitation functions for tensor polarization in π-d scattering measured at SIN (Grüebler *et al.*) and at LAMPF (present work). The curves represent recent calculations of Garcilazo (Ref. 22) and Matsuyama and Lee (Ref. 23).

B. Pion absorption

Pion absorption in nuclei has emerged as a major issue in medium-energy physics. Although many experiments involving the $\pi d \rightarrow NN$ reaction have been performed, the absorption process has not been explained adequately and the effect of pion absorption on the elastic amplitudes is poorly understood. In order to investigate further the effect of absorption on the elastic channel, it is essential to focus on the P_{11} π-N amplitude, since this amplitude is necessary for true pion absorption. Mizutani *et al.*[2] have emphasized that the decomposition of the P_{11} π-N amplitude into the pole and nonpole pieces is not known at present. The pole term is necessary for pion absorption while both amplitudes contribute to pion rescattering in the nucleus. Mizutani *et al.*[2] and Blankleider and Afnan[4] argue that experiments in π-N scattering give a measurement of the sum of these two terms only, while the relative strength of these two amplitudes is important in π-nucleus scattering. More recently, Garcilazo[22] argues that the P_{11} amplitude should be treated in the same manner as other π-N amplitudes in calculations of π-nucleus scattering. Previous experiments have imposed very little constraint on the pole and nonpole components of the P_{11} amplitude. However, measurements of t_{20}^{lab} in π-d scattering are expected to place an important restriction on the P_{11} amplitude and should help to settle the theoretical debate.

Presently, the theoretical calculations of the π-d system have achieved a high level of sophistication. These calculations are typically three-body in nature, include relativistic kinematics, and treat the pion-scattering $\pi d \rightarrow \pi d$ and pion-absorption $\pi d \rightarrow NN$ as coupled processes. The major difference among the calculations is the manner in which pion absorption is treated. In a phenomenological approach, Betz and Lee[3] use an effective interaction potential to describe the NN-ΔN transition by fitting NN-scattering phase shifts up to 800 MeV. In a more microscopic approach, the other authors explicitly incorporate the πNN and πNΔ coupling constants in the calculations. Blankleider and Afnan[4] include only π exchange between the nucleons and use relativistic kinematics only for the pions, while Rinat and Starkand[5] include both ρ and π exchange and treat the nucleons also relativistically. In the most recent calculation, Garcilazo[22] treats both the space and spin variables relativistically. Garcilazo claims that

there is no need to treat the nucleon pole term separately, since the effects of pion absorption on the elastic channel can be included correctly by using the experimental π-N P_{11} amplitude. This results in much smaller effects and gives the best agreement with the data achieved so far, not only for the tensor polarization t_{20} (see Fig. 10), but also for the vector polarization. Garcilazo concludes that the large effects obtained from pion absorption by the previous calculations[2,4-6] are spurious due to an incorrect decomposition of the P_{11} term into pole and nonpole pieces. A similar calculation in which the P_{11} pole term has not been isolated has been performed by Matsuyama and Lee.[23] The result of that calculation also agrees well with the present data as indicated in Fig. 10.

Angular distributions of t_{20} from the present work are shown in Fig. 11 for pion energies of 142, 180, 220, and 256 MeV. The results are compared with theoretical calculations of Betz and Lee,[3] Blankleider and Afnan,[4] Rinat and Starkand,[5] Fayard *et al.*,[6] and Garcilazo.[22] In addition, the dotted curves represent calculations[4-6] without the P_{11} π-N channel. Omitting this channel has the effect of removing absorption and P_{11} π-N rescattering from the calculation. While this is certainly not a realistic procedure, it gives nevertheless remarkably good agreement with the data. It is also noteworthy that the various theory groups get almost the same results from calculations without the P_{11} amplitude, while their full calculations differ by much more. This indicates that the biggest theoretical uncertainty is in the techniques used to include pion absorption.

The present data clearly indicate that the role of the P_{11} channel in determining π-d elastic scattering is quite different than that emphasized by most theoretical studies. Not only are the tensor polarization data well described if the P_{11} π-N channel is removed, but also cross sections and vector polarization data are best reproduced at low pion energies (Fig. 12). In addition, Afnan and Blankleider[24] have shown that true pion absorption can be expected to proceed primarily through the $L_{N\Delta}=0$ and $J^{\pi}=2^{+}$ channel, whereas the amplitude that is believed to have the dominant effect on the elastic channel has $L_{N\Delta}=2$, $J^{\pi}=0^{+}$. Thus, the elastic scattering data indicate that most theoretical treatments of the 0^{+} absorptive channel is in error, while no claim is made about the 2^{+} channel which gives rise to most of the true absorptive cross section.

C. Dibaryon resonances

The existence of dibaryon resonances was inferred from polarized proton-proton scattering experiments.[25] Later, possible evidence for dibaryon resonances was found in π-d elastic scattering cross sections,[8] in πd vector analyzing power measurements[10] at 256 MeV, and in πd tensor-polarization data at 134 MeV.[12] As discussed before, the present work shows no rapid energy dependence of the

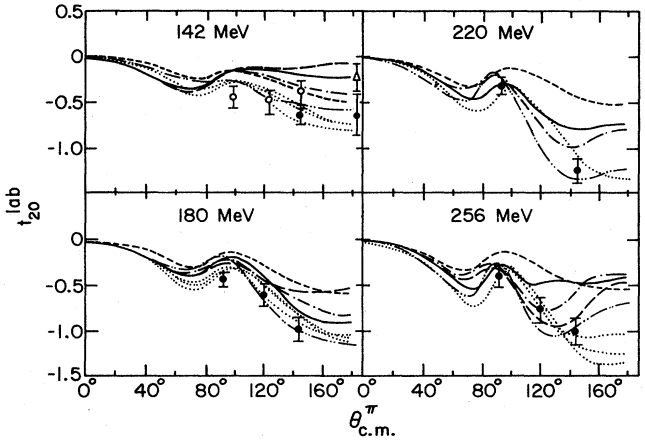

FIG. 11. Angular distributions at pion energies of 142, 180, 220, and 256 MeV. [Open circles and triangle are from the previous experiments (Refs. 9 and 13).] The calculations are from Blankleider and Afnan (Ref. 4) (——); Betz and Lee (Ref. 3) (----); Fayard, Lamot, and Mizutani (Ref. 6) (– –); Rinat and Starkand (Ref. 5) (–·–); and from Garcilazo (Ref. 22) (–··–), all including true pion absorption. The dotted lines are results without P_{11} amplitude, i.e., without pion absorption.

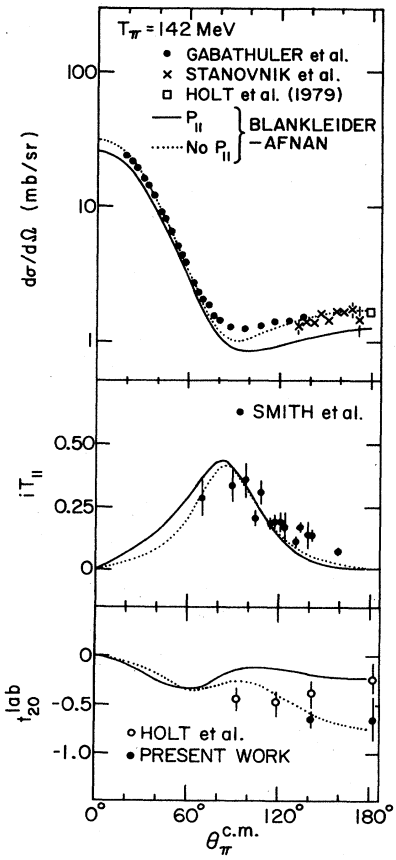

FIG. 12. Cross section, vector polarization, and tensor polarization data at 142 MeV compared with calculations from Blankleider and Afnan (Ref. 4), including (— — —) or omitting (···) the P_{11} amplitude.

tensor polarization and differs considerably from the SIN data[12] at 134 MeV. Meanwhile, newer and more precise measurements of the vector polarization[11] failed to confirm the early results[10] by the original group and found no oscillations at backward angles. Finally, recent $\pi d \rightarrow pp$ data exhibit[26] very smooth angular distributions and excitation functions. Therefore, there is little experimental evidence that dibaryon resonances are observed in low-energy πd scattering. Afnan and Blankleider[25] find that the intermediate NN channel with $L_{NN}=0$ dominates elastic scattering while channels with larger NN angular momentum have only a very weak influence. It is thus possible that effects of the proposed dibaryon resonances with $L_{NN}>0$ could be suppressed in elastic πd scattering at these energies. Evidently, the theoretical calculations need to be improved before this question can be settled.

D. Quadrupole form factor of the deuteron

The prospect of measuring the quadrupole form factor of the deuteron by observing t_{20} in π-d scattering was discussed very early[1] and led to an interest in measuring t_{20} near $\theta_d=0°$. The sensitivity of t_{20} to the quadrupole form factor can be seen readily from a simple expression based on an impulse approximation. The expression is given in terms of the π-N nonflip $g(\theta)$ and spin-flip $h(\theta)$ amplitudes as well as the ratio x of the quadrupole (F_2) to the monopole (F_0) form factor of the deuteron:

$$t_{20}=-(2)^{-1/2}\left[\frac{3|g|^2(2^{3/2}+x)x+|h|^2y^2}{3|g|^2(1+x^2)+2|h|^2y^2}\right],$$

where $x=F_2/F_0$ and $y=F_1/F_0$. Here, F_1 is the dipole form factor. At large scattering angles where $|g|^2 \gg |h|^2$, t_{20} is given by

$$t_{20}\approx-(2)^{-1/2}x\left[\frac{2^{3/2}+x}{1+x^2}\right],$$

and thus depends critically upon x, the ratio of the quadrupole to monopole form factor. It is this dependence that led several authors[1] to suggest that t_{20} in π-d scattering at an angle of 180° would provide a measurement of the deuteron D-state probability. Very soon, however, it became apparent that the calculated values of t_{20} in π-d scattering depend on the pion-absorption mechanisms[3–6] and that t_{20} varies strongly for different calculations. Therefore, it is likely that the quadrupole form factor F_2 or the ratio F_2/F_0 is better determined from a tensor polarization measurement in e-d scattering. However, if the absorption effects can be determined, then π-d scattering offers complementary information, particularly at high-momentum transfer.

IV. CONCLUSION

Together with previous cross section and vector polarization data, the new angular distribution of t_{20} at four energies allow for the first time a stringent test of the theoretical results. Older calculations do not predict the tensor polarization very well, in fact the best agreement is obtained when the P_{11} π-N amplitude is omitted altogether. This is certainly not an acceptable procedure, but it seems that the influence of pion absorption is overestimated. The results of several calculations that include absorption differ considerably from each other and from the data, with the exception of the most recent ones[22,23] which are in remarkably good agreement. In contrast to the earlier calculations, these most recent results do not treat the P_{11} nuclear pole term separately.

The present tensor polarization measurements exhibit no direct evidence for a dibaryon resonance. Since the present measurements indicate that the effects from pion absorption on the elastic channel should be small, it seems unlikely that dibaryon structures have a strong influence on π-d scattering. If the pion absorption effects are indeed small and if they can be calculated precisely, then perhaps the tensor polarization from π-d scattering can be used to measure the quadrupole form factor of the deuteron.

ACKNOWLEDGMENTS

We thank Dr. K. Stephenson, Dr. J. S. Frank, and Dr. M. J. Leitch for their substantial work in developing the new polarimeter. In addition, we thank Dr. B. Blankleider, Dr. W. R. Gibbs, Dr. B. F. Gibson, Dr. T.-S. H. Lee, and Dr. A. S. Rinat for very useful discussions and Dr. B. Blankleider, Dr. C. Fayard, Dr. A. S. Rinat, and Dr. H. Garcilazo for providing their results before publication. We are grateful to Dr. S. J. St. Lorant for the loan of the ^{3}He gas. This research was supported by the U.S. Department of Energy and the National Science Foundation.

*Present address: Institut für Mittelenergie Physik, Schweizerisches Institut für Nuklearforschung, Villigen, Switzerland.

†Present address: Fermi National Accelerator Laboratory, Batavia, IL 60510.

[1] W. R. Gibbs, Phys. Rev. C **3**, 1127 (1971); N. Giraud, Y. Avishai, C. Fayard, and G. H. Lamot, Phys. Lett. **77B**, 141 (1978); Phys. Rev. C **19**, 465 (1979).

[2] T. Mizutani, C. Fayard, G. H. Lamot, and S. Nahabetian, Phys. Rev. C **24**, 2633 (1981).

[3] M. Betz and T.-S. H. Lee, Phys. Rev. C **23**, 375 (1981).

[4] B. Blankleider and I. R. Afnan, Phys. Rev. C **24**, 1572 (1981).

[5] A. S. Rinat, E. Hammel, Y. Starkand, and A. W. Thomas, Nucl. Phys. **A329**, 285 (1975); A. S. Rinat and Y. Starkand, *ibid.* **A397**, 381 (1983).

[6] C. Fayard, G. H. Lamot, and T. Mizutani, Phys. Rev. Lett. **45**, 524 (1980).

[7] E. G. Pewitt, T. M. Fields, G. B. Yodh, J. G. Fetkovich, and M. Derrick, Phys. Rev. **131**, 1826 (1963); K. Gabathuler, J. Domingo, P. Gram, W. Hirt, G. Jones, P. Schwaller, J. Zichy, J. Bolger, Q. Ingram, J. P. Albanese, and J. Arvieux, Nucl. Phys. **A350**, 253 (1980); A. Stanovnik, G. Kernel, N. W. Tanner, T. Bressani, E. Chiavassa, S. Costa, G. Dellacasa, M. Gallio, A. Musso, M. Panighini, K. Bos, E. G. Michaelis, W. Van Doesburg, and J. D. Davies, Phys. Lett. **94B**, 323 (1980);

R. C. Minehart, J. S. Boswell, J. F. Davis, D. Day, J. S. McCarthy, R. R. Whitney, H. J. Ziock, and E. A. Wadlinger, Phys. Rev. Lett. **46**, 1185 (1981); T. G. Masterson, J. J. Kraushaar, R. J. Peterson, R. S. Raymond, R. A. Ristinen, R. L. Boudrie, E. F. Gibson, and A. W. Thomas, Phys. Rev. C **26**, 2091 (1982).

[8]R. Frascaria, I. Brissaud, J. P. Didelez, C. Perrin, J. L. Beveridge, J. P. Egger, F. Goetz, P. Gretillat, R. R. Johnson, C. Lunke, E. Schwarz, and B. M. Preedom, Phys. Lett. **91B**, 345 (1980).

[9]R. J. Holt, J. R. Specht, E. J. Stephenson, B. Zeidman, R. L. Burman, J. S. Frank, M. J. Leitch, J. D. Moses, M. A. Yates-Williams, R. M. Laszewski, and R. P. Redwine, Phys. Rev. Lett. **43**, 1229 (1979).

[10]J. Bolger, E. Boschitz, E. L. Mathie, G. R. Smith, M. Meyer, F. Vogler, S. Mango, J. A. Konter, G. S. Mutchler, and J. Arvieux, Phys. Rev. Lett. **48**, 1667 (1982); J. Bolger, E. Boschitz, G. Pröbstle, G. R. Smith, S. Mango, F. Volger, R. R. Johnson, and J. Arvieux, *ibid.* **46**, 167 (1981).

[11]G. R. Smith, E. L. Mathie, E. T. Boschitz, C. R. Otterman, S. Mango, J. A. Konter, M. Daum, M. Meyer, R. Olszewski, and F. Vogler, Phys. Rev. C (to be published).

[12]J. Ulbricht, V. König, W. Grüebler, P. A. Schmelzbach, B. Jenny, F. Sperisen, K. Elsener, C. Schweizer, and A. Chisholm, Phys. Rev. Lett. **48**, 311 (1982); W. Grüebler, J. Ulbricht, V. König, P. A. Schmelzbach, K. Elsener, C. Schweizer, M. Merdzan, and A. Chisholm, *ibid.* **49**, 444 (1982); V. König, A. Chisholm, W. Grüebler, J. Ulbricht, P. A. Schmelzbach, M. Merdzan, and K. Elsener, J. Phys. **9**, L211 (1983); V. König, W. Grüebler, J. Ulbricht, P. A. Schmelzbach, J. Donaldson, M. Merdzan, K. Elsener, D. Singy, and W. Z. Zhang, in *Proceedings of the Tenth International Conference on Few Body Problems in Physics, Karlsruhe, 1983,* edited by B. Zeitwitz (North-Holland, Amsterdam, 1984), p. 79.

[13]R. J. Holt, J. R. Specht, K. Stephenson, B. Zeidman, J. S. Frank, M. J. Leitch, J. D. Moses, E. J. Stephenson, and R. M. Laszewski, Phys. Rev. Lett. **47**, 472 (1981).

[14]E. Ungricht, W. S. Freeman, D. F. Geesaman, R. J. Holt, J. R. Specht, B. Zeidman, E. J. Stephenson, J. D. Moses, M. Farkhondeh, S. Gilad, and R. P. Redwine, Phys. Rev. Lett. **52**, 333 (1984).

[15]R. D. Werbeck and R. J. Macek, IEEE Trans. Nucl. Sci. **NS-22**, 156 (1975).

[16]B. J. Dropesky, G. W. Butler, C. J. Orth, R. Williams, M. A. Yates-Williams, G. Friedlander, and S. B. Kaufman, Phys. Rev. C **20**, 1844 (1979).

[17]E. J. Stephenson, R. J. Holt, J. R. Specht, J. D. Moses, R. L. Burman, G. D. Crocker, J. S. Frank, M. J. Leitch, and R. M. Laszewski, Nucl. Instrum. Methods **178**, 345 (1980).

[18]M. E. Schulze, D. Beck, M. Farkhondeh, S. Gilad, R. Goloskie, R. J. Holt, S. Kowalski, R. M. Laszewski, M. J. Leitch, J. D. Moses, R. P. Redwine, D. P. Saylor, J. R. Specht, E. J. Stephenson, K. Stephenson, W. Turchinetz, and B. Zeidman, Phys. Rev. Lett. **52**, 597 (1984).

[19]E. J. Stephenson, H. E. Conzett, R. M. Larimer, B. T. Leeman, R. Roy, and P. von Rossen, Phys. Rev. C **21**, 44 (1980); W. Grüebler, V. König, P. Schmelzbach, B. Jenny, H. R. Bürgi, R. A. Hardekopf, J. Nurzynski, and R. Risler, Nucl. Phys. **A334**, 365 (1980).

[20]W. Grüebler, V. König, A. Ruh, P. A. Schmelzbach, R. E. While, and P. Marmier, Nucl. Phys. **A176**, 631 (1971).

[21]The polarization is defined according to the Madison convention as given in *Polarization Phenomena in Nuclear Reactions,* edited by H. H. Barschall and W. Haeberli (University of Wisconsin, Madison, 1971), p. xxv.

[22]H. Garcilazo, Phys. Rev. Lett. **52**, 333 (1984).

[23]T. Matsuyama and T.-S. H. Lee (private communication).

[24]I. R. Afnan and B. Blankleider, Phys. Lett. **93B**, 367 (1980); Phys. Rev. C **22**, 1638 (1980).

[25]I. P. Auer, A. Beretvas, E. Colton, H. Halpern, D. Hill, K. Nield, B. Sandler, H. Spinka, G. Theodosiou, D. Underwood, Y. Watanabe, and A. Yokosawa, Phys. Rev. Lett. **41**, 1436 (1978).

[26]A. Saha, K. K. Seth, D. Kielczewska, S. Iversen, M. Kaletka, D. Barlow, and D. Smith, Phys. Rev. Lett. **51**, 759 (1983).